



Producing ZnFe₂O₄ thin films from ZnO/FeO multilayers

Karen L. Salcedo Rodríguez^{a,*}, Martin Hoffmann^{b,c}, Federico Golmar^{d,e},
Gustavo Pasquevich^{a,f}, Peter Werner^g, Wolfram Hergert^c, Claudia E. Rodríguez Torres^a

^a IFLP y Departamento Física, Facultad de Ciencias Exactas, Universidad Nacional de la Plata-CCT La Plata CONICET, C.C. 67, CP 1900 La Plata, Argentina

^b IFW Dresden, P.O. Box 270116, D-01171 Dresden, Germany

^c Institute for Physics, Martin Luther University Halle-Wittenberg, Von-Seckendorff-Platz 1, 06120 Halle (Saale), Germany

^d CIC nanoGUNE, 20018 Donostia-San Sebastian, Basque Country, Spain

^e I.N.T.I.-CONICET and ECyT-UNSAM, San Martín, Bs. As., Argentina

^f Departamento de Ciencias Básicas, Facultad de Ingeniería, Universidad Nacional de La Plata, CP 1900 La Plata, Argentina

^g Max Planck Institute of Microstructure Physics, Weinberg 2, D-06120 Halle (Saale), Germany

ARTICLE INFO

Article history:

Received 7 June 2016

Received in revised form

15 September 2016

Accepted 19 September 2016

Available online 23 September 2016

Keywords:

ZnFe₂O₄

DC-sputtering

Cation inversion

Spin glass

ABSTRACT

The present work investigates the structural and magnetic properties of ZnFe₂O₄ thin films obtained from ZnO/FeO multilayers deposited on MgO substrate by DC reactive sputtering. We show that this method is good to grow efficiently ordered ZnFe₂O₄ films. The quality of the thin films is ensured by TEM measurements, which showed a well ordered film of ZnFe₂O₄. The magnetic properties of these thin films present still minimal differences when compared to bulk ZnFe₂O₄ powders. They exhibit a ferromagnetic-like behavior at low temperatures, whereas ZnFe₂O₄ is expected to be antiferromagnetic. We found that the magnetic signal originated from the film surface, where cation inversion was visible from grazing incidence X-ray fluorescence measurements. The inversion of Fe ions with Zn ions caused a magnetic spin glass state, which created then the ferromagnetic-like behavior differently to bulk ZnFe₂O₄. These facts point to possible routes in order to improve the growing process of ZnFe₂O₄ via ZnO/FeO multilayers.

© 2016 Elsevier B.V. All rights reserved.

1. Introduction

Zinc ferrite, ZnFe₂O₄, captured scientific interests for many years because of interesting magnetic properties compared with other spinel ferrites and its application as transparent magnetic semiconductor [1].

In the perfect case, bulk ZnFe₂O₄ forms a normal spinel structure, in which the zinc ions (Zn²⁺) occupy the tetrahedral (A) sites and iron ions (Fe³⁺) occupy the octahedral (B) sites. It shows an antiferromagnetic (AFM) order below the Néel temperature, $T_N = 10.5\text{K}$ [2], which is driven by an oxygen-mediated superexchange between the Fe³⁺ ions located at B sites. However, it is well known that small scale changes in the ordering of the Fe ions can also influence the magnetic properties on the macroscopic level. The AFM order can be turned into a ferrimagnetic behavior at room temperature for nano-structured ZnFe₂O₄ systems, e.g., thin films or nanoparticles [3,4]. The ferrimagnetism is thereby mainly attributed to cation inversion, i.e., Zn and Fe ions might occupy both types of sites (A and B sites). However, other kinds of structural

defects like oxygen vacancies can also influence the magnetic order [5,6]. Thus, all these variations of the structural and magnetic properties in ZnFe₂O₄ depend strongly on the preparation technique used to obtain the ZnFe₂O₄ samples [1,7–9]. Another route to grow high quality ZnFe₂O₄ thin films was recently reported by us using magnetron sputtering to grow a series of epitaxial ZnO/FeO multilayers [9]. The advantages of this method are the usage of metallic targets while no RF power supply is needed. The used DC power is easy to control and represents a low cost option. We found in the X-ray diffraction patterns and in the magnetic properties of the thin films [9] clear indications for pure ZnFe₂O₄ but at small temperatures the hysteresis curve and the zero field and field cooled magnetization versus temperature curves showed an anomalous magnetic behavior with respect to the magnetic response of a ZnFe₂O₄ powder sample [9]. The samples with the highest number of multilayers (20 ZnO/FeO bilayers) appeared to have the best agreement with the properties of ZnFe₂O₄. Thus, we took those samples in order to characterize intensively their film quality and explore the origin of the remaining magnetic response. Therefore, we complemented our previous results with an extensive study of the local composition inside the layer and at its surface by applying X-ray absorption near edge spectroscopy (XANES), extended X-ray absorption fine structure spectroscopy (EXAFS) and

* Corresponding author.

E-mail address: klsalcedor@fisica.unlp.edu.ar (K.L. Salcedo Rodríguez).

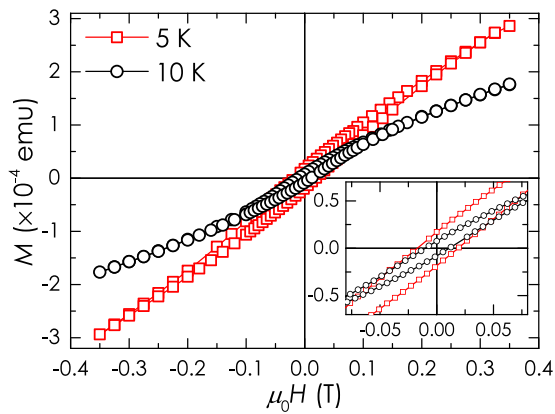


Fig. 1. Magnetization of the thin film (ZFO-TF) as a function of the applied field, H , at 5 K and 10 K. Both curves show a pronounced hysteresis loop. See the inset for an amplification of the low field region.

grazing incidence X-ray fluorescence (GI-XRF) measurements [10]. By the measurement of fluorescence signals at various incidence angles, the GI-XRF provides information about the depth distribution of the elements in the layer. This technique is even at depths of few nanometers very sensitive and provides in combination with XANES an interesting method in order to relate the thickness-dependent electronic structure with magnetic properties. Thereby, we can explain that the variation of the magnetic properties with respect to ZnFe_2O_4 powder originates only from a cation inversion at the surface of the films. The magnetic moments in this small fraction of the sample behave then like a spin glass.

2. Experimental

2.1. Samples

The epitaxial ZnFe_2O_4 films have been grown on a $\text{MgO}(001)$ substrate from ZnO/FeO multilayers [9]. We started from Zn and Fe metal targets in oxygen atmosphere by DC magnetron sputtering. Two samples were grown simultaneously. These consist of 20 bilayers of a 1.6 nm ZnO film and a 3.1 nm FeO film, starting at the interface with an FeO layer. These films show similar structural and magnetic properties as the samples Z20 used before [9]. Therefore, we group them together under the term ZnFe_2O_4 -thin film (ZFO-TF) hereafter.

The corresponding thicknesses were calculated taking into account the deposition velocities of FeO and ZnO under the same experimental conditions. The expected total thickness of the film is 94 nm. The multilayers were grown with a base pressure of 2×10^{-7} Torr and an operation pressure of 2×10^{-2} Torr under Ar and O_2 atmosphere with a flux of 22 ml/min and 3 ml/min, respectively. The supplied DC power was 200 W. The deposition itself was carried out at a substrate temperature of 973 K in order to enhance the interlayer diffusion. We compared the properties of the thin films with a sample of bulk ferrite powder (ZFO-P). ZFO-P was prepared by conventional solid state reaction, therein, Fe_2O_3 and ZnO were mixed in an agate mortar with a ratio of 1:1. This mixture was calcinated at 1000 °C for 12 h. The process was repeated three times.

2.2. Chemical and structural characterization

The chemical composition of the sample was obtained by energy dispersive X-ray spectrometry (EDX), which was carried out at 5 kV and 10 kV acceleration voltages. We used a focused ion beam (FIB), model “Nanolab 650”, equipped with an energy dispersive X-ray

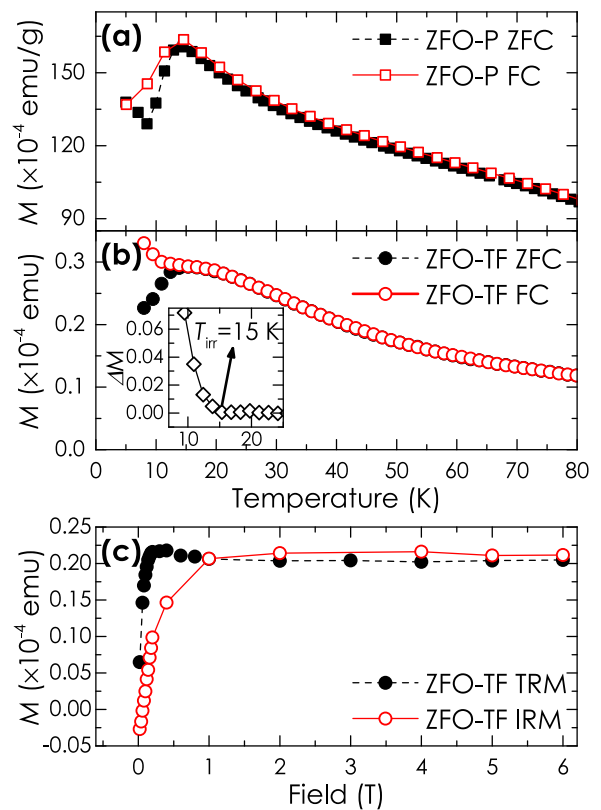


Fig. 2. Zero field cooled and field cooled measurements (M vs T) at 500 Oe for (a) bulk ZnFe_2O_4 reference and (b) ZFO-TF sample. The inset in (b) shows the irreversibility, ΔM , between FC and ZFC curves for ZFO-TF indicating the point of separation with the temperature, T_{irr} (c) TRM and IRM measurements for the ZFO-TF samples.

spectrometer, model Apollo X. The morphology of the samples was characterized through atomic force microscopy by a NT-MDT SMENA Solver-PRO using a tapping mode. The analysis was performed by means of the Nova Image Analysis program interface NT-MDT. The crystal structure of the deposited layers was analyzed by Conventional transmission electron microscopy (TEM), high-resolution TEM (HREM) as well as by scanning transmission electron microscopy (STEM). We used a TITAN 80/300 from FEI working at an acceleration voltage of 300 kV. The STEM was also equipped with an EDX spectrometer in order to get an element analysis (line scans as well as 2D mapping). For these investigations, cross-sections of the films have been prepared by conventional techniques (slicing, dimpling, ion-milling). Note that we had two EDX spectrometer, one within the FIB and the other within the STEM measuring setup.

2.3. Magnetic characterization

Magnetic measurements were performed using a Quantum Design magnetometer superconducting quantum interference device (SQUID) magnetometer. The magnetization, M , was measured as a function of temperature, T , and the zero field cooled (ZFC) and field cooled (FC) measurements were carried out between 5 K and 300 K at a field of 50 Oe. The thermoremanent magnetization (TRM) and the isothermoremanent magnetization (IRM) data are also collected. TRM measurement is performed cooling the sample from RT down to 5 K at a constant H_{TRM} magnetic field between 0 and 6 Tesla. Afterwards, the magnetic field is removed and the remanent magnetizations are measured as fast as possible. In the case of IRM measurements, the sample was cooled in zero applied field from room temperature down to 5 K. Afterwards, the field was

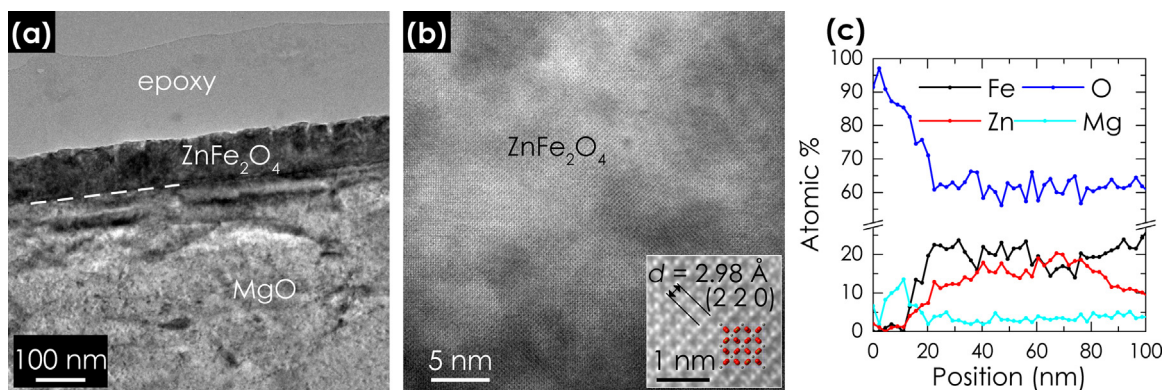


Fig. 3. (a) TEM cross section image, (b) HRSTEM image, and (c) EDX atomic profile of the ZnFe_2O_4 thin film (ZFO-TF).

momentarily applied for 120 s (same fields as for TRM), removed again, and the remanent magnetization was recorded.

2.4. X-ray measurements at LNLS (Campinas, Brazil)

GI-XRF measurements were performed at the XRF fluorescence beamline, using a monochromatic X-ray beam of 9.7 keV. Angular scans between 0° and 1° were performed. This angular range included the total-reflection critical-angle. The XANES Fe K-edge (7112 eV) and Zn K-edge (9659 eV) spectra were collected, in fluorescence mode, for grazing angles below and above the critical-angle, using a Si(111) channel-cut monochromator. In addition, conventional XANES and EXAFS spectra at the Zn and Fe K-edge were collected at the XAFS2 beamline at room temperature and in fluorescence mode while the sample was positioned 60° to the incoming X-ray beam.

3. Results and discussion

We have seen in our previous study [9] from the X-ray diffraction spectra that our method provides an epitaxial growth of zinc ferrite (100) on the MgO(100) substrate. On the other hand, we observe at low temperatures a ferromagnetic-like component instead of the expected antiferromagnetic behavior (Fig. 1).

The differences between the thin films and bulk ZnFe_2O_4 become in particular evident from the M versus T measurements (Fig. 2a and b). While the ZFC and FC curves almost coincide for bulk ZnFe_2O_4 presenting a maximum at 15 K and an inflexion point at 11 K (Fig. 2a; in agreement with the reported Neel temperature), for ZFO-TF, both curves become different below 15 K with an irreversibility temperature, $T_{\text{irr}} = 15.35$ K (Fig. 2b with the inset). For

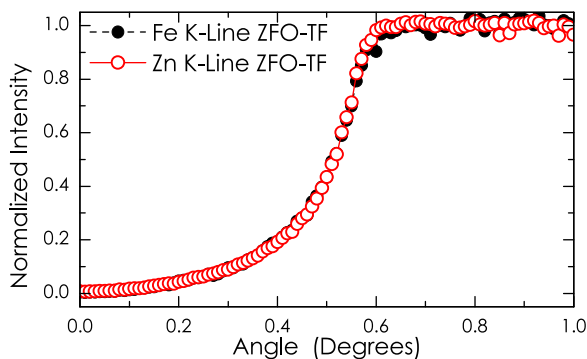


Fig. 4. Normalized intensity of Fe and Zn K-lines as a function of the incident angle of the angular scan GI-XRF measurements. Both intensities were normalized to their maximum value. The intensity jump around 0.5° corresponds to the total reflection condition.

the latter, the curves show a prominent convex shape around the maximum and afterwards a significant deviation, ΔM , between ZFC and FC signal, which was already reported to show the formation of a frustrated spin system in powdered ferrite monocrystals [11].

The irreversibility ΔM (inset in Fig. 2b) identifies the magnetic character of the system as a spin glass (SG), superparamagnetism (SPM) or diluted antiferromagnetism in an applied field (DAFF). The latter consists of small ferromagnetic clusters enclosed in an antiferromagnetic matrix [12–14].

In order to distinguish between the three possible scenarios, we analyze TRM and IRM measurements. They represent a

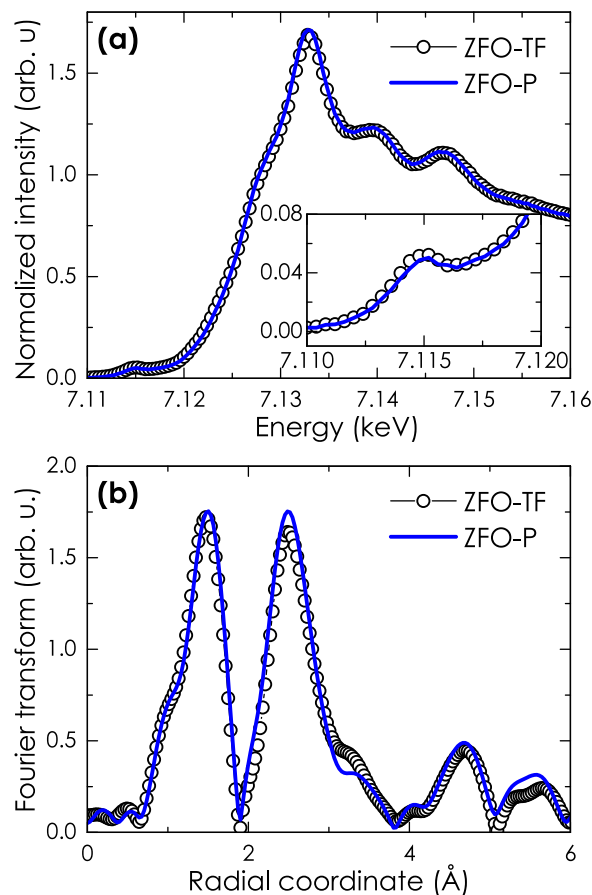


Fig. 5. (a) Measured XANES spectra at Fe K-edge of ZFO-TF (open circles) and ZFO-P (solid line). The incidence angle was of 60° . The inset shows a zoom into the prepeak region. (b) Fourier transform of the EXAFS oscillations at the Fe K-edges of ZFO-TF (open circles) and the ZFO-P (solid line).

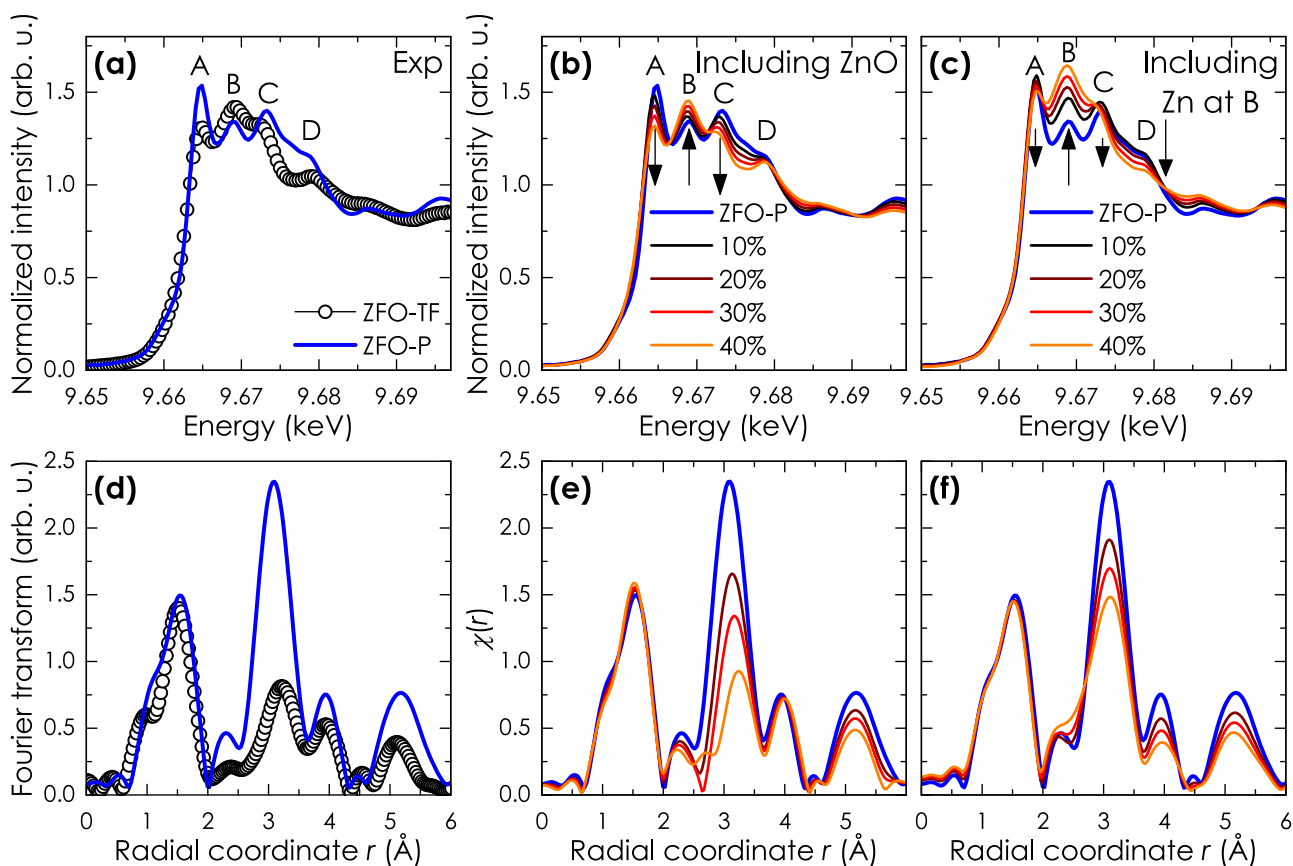


Fig. 6. (a) Measured XANES spectra at the Zn K-edge of ZFO-TF (open points) and bulk ZFO-P (solid line). The incidence angle was 60° . (b) and (c) theoretical simulations of the XANES spectra at the Zn K-edge considering the effect of different percentages of co-existing (b) ZnO or (c) Zn at A and B sites within the ZFO film. Arrows indicated the tendencies of feature changes in the white line of the XANES spectra in each case. (d) Fourier transform of the EXAFS oscillation measured at the Zn K-edges of ZFO-TF (open points) and ZFO-P (solid line). (e) and (f) theoretical simulations of the Fourier transform, considering the effect of different percentages of co-existing (e) ZnO or (f) Zn at A and B sites within the ZFO film.

useful method to identify the nature of the irreversible magnetization contributions [14–16]. For an ideal AFM bulk system, the TRM and IRM signals are expected to be zero for all fields and temperatures. The DAFF systems are characterized by zero IRM and with an applied field increasing TRM. In contrast, IRM increases in a system with SPM relatively strongly with increasing field and meets the TRM curve at moderate field values, where both curves saturate. A SG system shows a similar behavior but TMR increases steeply with the field and exhibit a characteristic peak at intermediate fields. Exactly the latter case is realized for our sample ZFO-TF (Fig. 2c). This is not surprising, since magnetic disorder is in general very common for ferrites. The disorder may cause a competition between the super exchange interactions J_{AB} , J_{AA} , and J_{BB} (magnetic exchange interactions between sites A–B, A–A, and B–B) and consequently frustration between the magnetic moments of the Fe ions. If for example the concentration of magnetic ions at the A site is sufficiently diluted, a spin glass state can be formed [17].

Thus, the exact chemical composition and the cation distribution was studied to understand the origin of the SG behavior.

The previous X-ray diffraction results [9] were complemented by TEM measurements. A cross-sectional TEM image reveals a dense and flat ZnFe_2O_4 film with no appreciable imperfections (Fig. 3a). The total thickness of the layer is 98 ± 4 nm, which is in very good agreement with the prediction from the deposition velocity. The complete interdiffusion of the epitaxial FeO/ZnO multilayers and hence an ordered atomic arrangement was also observed (Fig. 3b).

This interdiffusion is also verified by the EDX profile along the thin film obtained within the STEM measuring setup (Fig. 3c). The latter results allow to access an average atomic ratio, which is $\text{Fe}/\text{Zn} = 1.7 \pm 0.5$. These results agree well with the EDX spectrum from the FIB measuring setup. However, we observe in the EDX profile a higher concentration of Zn close to the substrate indicating a possible substitution of Mg atoms in MgO by Zn (Fig. 3c). This migration could be induced by the substrate temperature in the growing process, the similar atomic radii of Mg and Zn atoms (145 pm or 142 pm), or the same oxidation state. The grain size and the roughness of the sample was determined by means of atomic force microscopy and was about 118 nm and 3.4 nm, respectively, whereas the roughness of the MgO substrate was 2.34 nm. The homogeneous distribution of Fe and Zn atoms along the depth of the layers is also verified by the normalized fluorescence intensity of the Fe and Zn K lines (Fig. 4). The absence of oscillations indicates the mixture between the original ZnO/FeO multilayers in good agreement with the TEM result. In summary, we found with our extended structural analysis a homogeneous distribution of Fe and Zn ions in a $\text{ZnFe}_2\text{O}_4(100)$ thin film as before [9].

Therefore, we studied the microscopic chemical composition with XANES and EXAFS measurements, which yield information of the whole film, if the incidence angle is 60° . When we compare the XANES spectrum and the Fourier Transform (FT) of the EXAFS oscillations at the Zn K-edges for ZFO-TF with a reference ZnFe_2O_4 sample the differences between both at the Fe K-edge are negligible (Fig. 5a and b). In contrast, relevant differences appear in the case of the Zn K-edge (Fig. 6a). We observe a decrease of

the intensities of the first and the third peak (called A and C, respectively) and an increase in the intensity of the second characteristic peak (B). Regarding the FT, the one corresponding to ZFO-TF presents a notable decrease of the peak which corresponds to the second coordination layer (Fig. 6d). These changes at the K-edge, in XANES and FT, has been previously assigned to the occurrence of cations inversion [18,19], but the very good agreement of ZFO-TF and bulk ZnFe_2O_4 at the Fe K-edge allows us to conclude that the current environment of the Fe ions corresponds to that found in normal Zn ferrite. Thus, cation inversion, in the sense of Fe and Zn ions swapping sites, can be excluded within our thin films.

In order to understand the observed differences at the Zn K-edge, we take into account the higher Zn ion concentration at the interface and the non stoichiometric amount of Zn ions discussed above within the characterization of the chemical composition. These additional Zn ions might either occupy B sites or segregate as ZnO. Hence, we performed simulations of the XANES spectrum and the FT at the Zn K-edge in two different ways. We assumed (1) a mixture of Zn ferrite and ZnO, and (2) a mixture of Zn ions at A and B sites on $\text{Zn}_{1+x}\text{Fe}_{2-x}\text{O}_4$, where the excess of Zn relative to 1 is occupying B sites. In the first case, mixture of normal ZnFe_2O_4 Ferrite and ZnO spectra were simulated by simple superposition of individual experimental spectra, with a molar fraction of OZn in the range of 10–40%. The experimental spectrum of ZnFe_2O_4 were also used in case (2) as the reference XANES spectrum of a Zn ion at the A site. The simulation of the XANES spectrum of varying amounts of Zn ions at the B site was performed by means of the FDMNES code [20], whereas the Artemis code [21] was used for the FT signal.

We observe for the XANES spectra a similar effect in both models, a decreasing intensity of the A and C peak combined with an increased intensity of the B peak (Fig. 6b and c). The differences between the two models can be seen in the shape of shoulder called D. In the case of ZnO segregation, the shoulder becomes a well-defined peak while it decreases in the case of Zn ions at the B site.

Regarding the FT simulations, we observe that both models influence the intensity of the second peak centered at 3.1 \AA (Fig. 6e and f). Possible differences can be obtained in the third peak, which decreases for the case of Zn ions at B sites, but remains almost the same in the case of the mixture with ZnO. Thus, we cannot completely exclude one of the potential scenarios when comparing the simulated FT signals with the measurements for ZFO-TF (Fig. 6d). Therefore, taking into account that a perfect ZnFe_2O_4 lattice structure was identified within the HRSTEM images and the X-ray diffraction measurements, and that we did not find any region of ZnO, we can conclude that the growth of ZnFe_2O_4 from ZnO/FeO multilayers causes in within the thin films no cation inversion but the additional occupation of B sites by Zn ions.

On the other hand, the occupation of A and B sites by Zn ions does not cause a magnetic contribution [6]. Another possible source of magnetism could be originated in a quite small surface region showing nevertheless cation ion inversion, which was not traceable over the full width of the film. Such phenomenon was already observed, e.g., in MgAl_2O_4 , where cation inversion at the surface is the stable state [22]. It is driven by the need to rearrange charges in the surface layer to compensate the surface polarity. Thus, cation inversion might redistribute a substantial amount of cations at the surface of the spinel structure placing, e.g., Fe^{3+} ions in A and B sites. A selective information from the surface (depth of around 2–5 nm) are accessible via XANES spectra with a incidence angle of 0.4° (grazing incidence). Our results for the Zn K-edge present again the characteristics that can be assigned to Zn ions at A and B sites or ZnO precipitation – decreasing intensities of the first and third peak (A and C, respectively) and an increasing intensity in the second characteristic peak (B) (Fig. 7a). We found the best

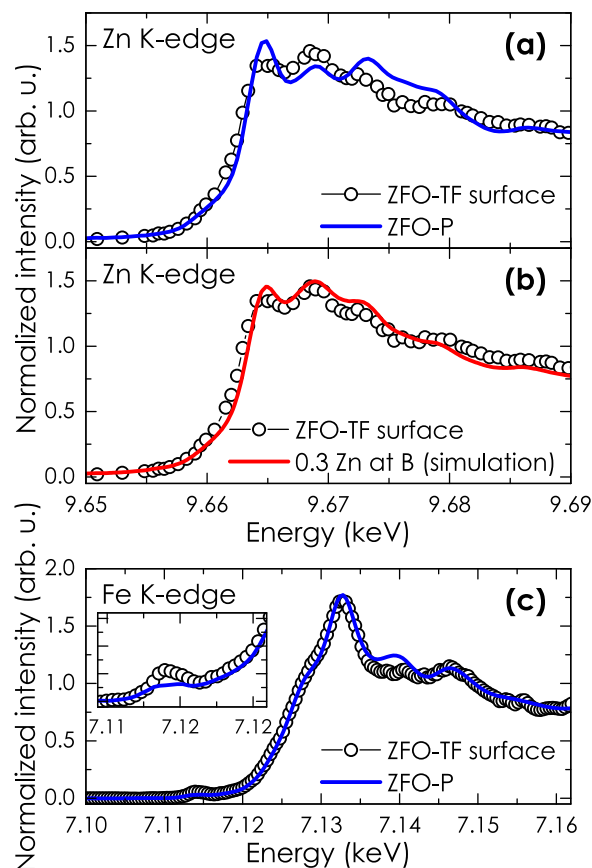


Fig. 7. (a) The XANES spectrum of ZFO-TF and ZFO-P measured at the Zn K-edge with grazing incidence (surface information). (b) Measured and simulated ZFO-TF spectra. The latter assumes 30% Zn in B site and 70% of Zn in A site. (c) Fe K-edge spectrum of ZFO-TF and ZFO-P measured with grazing incidence (surface information). The inset shows the zoom into the prepeak region.

agreement between the superficial XANES spectrum and the simulated one for a co-existence of 30% Zn ions at the B site and 70% Zn ions at the A site (Fig. 7b). On the other hand, the XANES spectrum at the Fe K-edge presented now – opposite to the case of the whole thin film – significant differences when compared to bulk ZnFe_2O_4 (Fig. 7c). We measured a decrease of the white line amplitude and an increase of pre-peak intensity. These features have been previously reported when some Fe atoms occupy non-centrosymmetric A sites instead of the centrosymmetric octahedral B sites [18,23]. Hence, the surface of the thin films presents cation inversion.

4. Conclusions

In our measurements, we demonstrate for the Zn ferrite thin films, obtained from epitaxial growth of ZnO/FeO multilayers by DC Magnetron sputtering, a slight Zn overstoichiometry, where the Zn ions occupy mainly additional B sites and do not influence the overall structural and magnetic properties of the thin films. The additional Zn ions are mainly located in the interface region close to the substrate. The local environment of the Fe^{3+} ions is within the thin film the same as in normal ZnFe_2O_4 (Fe at the octahedral B sites) but shows clear signals of cation inversion at the surface where Fe occupy A and B sites. The presence of iron at both sites explains the small magnetic signal at low temperatures below 30 K and the spin glass behavior. This magnetic order originates therefore only from the surface of the thin film. In summary, we found two main issues when growing ZnFe_2O_4 thin films from ZnO/FeO multilayers – Zn overstoichiometry and insufficient

surface quality. Only the latter can alter the magnetic response of ZnFe_2O_4 . Both problems can be optimized within the growing process. Thus, ZnO/FeO multilayers are an interesting method with the high potential of growing highly ordered ZnFe_2O_4 thin films.

Acknowledgements

This work is financially supported by the German Academic Exchange Service (DAAD) and the Ministry of Science, Technology and Productive Innovation of the Republic of Argentina, by means of the scientific project: “Experimental and theoretical Investigations of defect induced ferromagnetism at room temperature in Ferrites” (Project ID: 57052290 or DA13/02 MINCYT); Brazilian Synchrotron Light Laboratory-LNLS (proposals XAFS-14167 and XRF-101118), UNLP X543 and CONICET-PIP 112. It was partially funded by the *Deutsche Forschungsgemeinschaft* (DFG) within the SFB 762, “Functionality of Oxide Interfaces”. The authors thank Dr. Silvana J. Stewart (National University of La Plata, Bs.As, Argentina) for the preparation of the ZnFe_2O_4 bulk powder sample and Mrs. S. Hopfe (Max Plank Institute of Microstructure Physics, Halle, Germany) for the TEM sample preparation.

References

- [1] Y.F. Chen, D. Spoddig, M. Ziese, Epitaxial thin film ZnFe_2O_4 : a semi-transparent magnetic semiconductor with high Curie temperature, *J. Phys. D: Appl. Phys.* 41 (20) (2008) 205004, <http://dx.doi.org/10.1088/0022-3727/41/20/205004>.
- [2] W. Schiessl, W. Potzel, H. Karzel, M. Steiner, G.M. Kalvius, A. Martin, M.K. Krause, I. Halevy, J. Gal, W. Schafer, G. Will, M. Hillberg, R. Wäppling, Magnetic properties of the ZnFe_2O_4 spinel, *Phys. Rev. B* 53 (14) (1995) 9143–9152.
- [3] C. Jesus, E. Mendonça, L. Silva, W. Folly, C. Meneses, J. Duque, Weak ferromagnetic component on the bulk ZnFe_2O_4 compound, *J. Magn. Magn. Mater.* 350 (2014) 47, <http://dx.doi.org/10.1016/j.jmmm.2013.09.025>.
- [4] S. Nakashima, K. Fujita, K. Tanaka, K. Hirao, High magnetization and the high-temperature superparamagnetic transition with intercluster interaction in disordered zinc ferrite thin film, *J. Phys. Condens. Matter* 17 (1) (2005) 137, <http://dx.doi.org/10.1088/0953-8984/17/1/013>.
- [5] C.E. Rodríguez Torres, F. Golmar, M. Ziese, P. Esquinazi, S.P. Heluani, Evidence of defect-induced ferromagnetism in ZnFe_2O_4 thin films, *Phys. Rev. B: Condens. Matter* 84 (6) (2011) 064404, <http://dx.doi.org/10.1103/PhysRevB.84.064404>.
- [6] C.E. Rodríguez Torres, G.A. Pasquevich, P.M. Zélis, F. Golmar, S.P. Heluani, S.K. Nayak, W.A. Adeagbo, W. Hergert, M. Hoffmann, A. Ernst, P. Esquinazi, S.J. Stewart, Oxygen-vacancy-induced local ferromagnetism as a driving mechanism in enhancing the magnetic response of ferrites, *Phys. Rev. B* 89 (2014), <http://dx.doi.org/10.1103/PhysRevB.89.104411>.
- [7] A. Raghavender, Room temperature ferromagnetism in laser ablated Zn ferrite thin films, *Mater. Lett.* 65 (23–24) (2011) 3636, <http://dx.doi.org/10.1016/j.matlet.2011.08.005>.
- [8] J. Takaobushi, H. Tanaka, T. Kawai, S. Ueda, J.-J. Kim, M. Kobata, E. Ikenaga, M. Yabashi, K. Kobayashi, Y. Nishino, D. Miwa, K. Tamasaku, T. Ishikawa, $\text{Fe}_{3-x}\text{Zn}_x\text{O}_4$ thin film as tunable high Curie temperature ferromagnetic semiconductor, *Appl. Phys. Lett.* 89 (24) (2006) 242507, <http://dx.doi.org/10.1063/1.2405389>.
- [9] K.L. Salcedo Rodríguez, F. Golmar, C.E. Rodríguez Torres, Magnetic properties of Zn-ferrites obtained from multilayer film deposited by sputtering, *IEEE Trans. Magn.* 49 (8) (2013) 4559, <http://dx.doi.org/10.1109/TMAG.2013.2260529>.
- [10] M. Newville, Fundamentals of X-ray Absorption Fine Structure, Consortium for Advanced Radiation Sources, University of Chicago, USA, 2004 <http://xafs.org>.
- [11] T. Usa, K. Kamazawa, H. Sekiya, S. Nakamura, Y. Tsunoda, K. Kohn, M. Tanaka, Magnetic properties of ZnFe_2O_4 as a 3-D geometrical spin frustration system, *J. Phys. Soc. Jpn.* 73 (2004) 2834, <http://dx.doi.org/10.1143/JPSJ.73.2834>.
- [12] P. Miltényi, M. Gierlings, J. Keller, B. Beschoten, G. Güntherodt, U. Nowak, K.D. Usadel, Diluted antiferromagnets in exchange bias: proof of the domain state model, *Phys. Rev. Lett.* 84 (18) (2000) 4224, <http://dx.doi.org/10.1103/PhysRevLett.84.4224>.
- [13] U. Nowak, K.D. Usadel, J. Keller, P. Miltényi, B. Beschoten, G. Güntherodt, Domain state model for exchange bias. I. Theory, *Phys. Rev. B* 66 (1) (2002) 014430, <http://dx.doi.org/10.1103/PhysRevB.66.014430>.
- [14] M.J. Benitez, O. Petravic, E.L. Salabas, F. Radu, H. Tüysüz, F. Schüth, H. Zabel, Evidence for core-shell magnetic behavior in antiferromagnetic Co_3O_4 nanowires, *Phys. Rev. Lett.* 101 (9) (2008).
- [15] M.J. Benitez, O. Petravic, H. Tüysüz, F. Schüth, H. Zabel, Fingerprinting the magnetic behavior of antiferromagnetic nanostructures using remanent magnetization curves, *Phys. Rev. B* 83 (13) (2011) 134424, <http://dx.doi.org/10.1103/PhysRevB.83.134424>.
- [16] P. Nordblad, L. Lundgren, L. Sandlund, Field dependence of the remanent magnetization in spin glasses, *Europhys. Lett.* 3 (2) (1987) 235, <http://dx.doi.org/10.1209/0295-5075/3/2/017>.
- [17] J. Dumas, C. Schlenker, J.L. Tholence, R. Tournier, Spin-glass properties of a crystalline transition-metal oxide: $(\text{Ti}_{1-x}\text{V}_x)_2\text{O}_3$, *Phys. Rev. B* 20 (1979) 3913, <http://dx.doi.org/10.1103/PhysRevB.20.3913>.
- [18] S.J. Stewart, S.J.A. Figueroa, J.M. Ramallo López, S.G. Marchetti, J.F. Bengoa, R.J. Prado, F.G. Requejo, Cationic exchange in nanosized ZnFe_2O_4 spinel revealed by experimental and simulated near-edge absorption structure, *Phys. Rev. B* 75 (2007) 073408, <http://dx.doi.org/10.1103/PhysRevB.75.073408>.
- [19] S.J.A. Figueroa, S.J. Stewart, First XANES evidence of a disorder-order transition in a spinel ferrite compound: nanocrystalline ZnFe_2O_4 , *J. Synchrotron. Radiat.* 16 (2009) 63, <http://dx.doi.org/10.1107/S0909049508032433>.
- [20] O. Bunu, Y. Joly, Self-consistent aspects of X-ray absorption calculations, *J. Phys. Condens. Matter* 21 (34) (2009) 345501, <http://dx.doi.org/10.1088/0953-8984/21/34/345501>.
- [21] URL: <http://cars.uchicago.edu/ifeffit>.
- [22] M.K. Rasmussen, A.S. Foster, B. Hinnemann, F.F. Canova, S. Helveg, K. Meinander, N.M. Martin, J. Knudsen, A. Vlad, E. Lundgren, A. Stierle, F. Besenbacher, J.V. Lauritsen, Stable cation inversion at the MgAl_2O_4 spinel surface, *Phys. Rev. Lett.* 107 (2011) 036102, <http://dx.doi.org/10.1103/PhysRevLett.107.036102>.
- [23] V. Blanco-Gutiérrez, F. Jiménez-Villacorta, P. Bonville, M.J. Torralvo-Fernández, R. Sáez-Puche, X-ray absorption spectroscopy and Mössbauer spectroscopy studies of superparamagnetic ZnFe_2O_4 nanoparticles, *J. Phys. Chem. C* 115 (5) (2011) 1627, <http://dx.doi.org/10.1021/jp109368z>.